Calibration of an MR-Compatible, CZT Detector Based Stationary Small Animal SPECT system

Andrew Rittenbach[1], Jingyan Xu[1], AbdEl-Monem El-Sharkawy[1], William Edelstein[1], Kevin Parnham[2], James Hugg[2], Benjamin M. W. Tsui[1]

[1]Johns Hopkins University, Baltimore MD, USA
[2]Gamma Medica Inc., Northridge CA, USA

JOHNS HOPKINS MEDICINE
SCHOOL OF MEDICINE

Outline

- Objective
- Background
  - Description of the small animal SPECT system
  - Importance of system calibration
- Method
  - Geometric calibration
  - Energy calibration
  - Uniformity calibration
  - Calibration evaluation experiments
- Results
  - Effect of geometric calibration
  - Effect of energy calibration
  - Effect of uniformity calibration
- Conclusion

Objective

- To develop a simple system calibration method for a ring-type CZT based SPECT insert to be used for small animal SPECT-MR imaging
  - Our system calibration method must
    - Measure any misalignment between collimator and detector
    - Identify energy peak and measure energy resolution for each detector pixel
    - Correct for detector uniformity due to property variations of different detector pixels
    - Identify and correct for malfunctioning detector pixels

SPECT System Description

- The small animal SPECT system consists of 95 CZT detector modules backed by MR compatible ASIC electronics
  - Each detector module consists of 16 x 16 pixels, with side length of 1.6mm
  - There are 5 contiguous rings consisting of 19 detector modules
  - The 95 CZT detector modules form a seamless detector surface with 24320 pixels

Single MR-compatible CZT detector module with ASIC

SPECT system with 5 rings of 19 CZT detector modules and with cover removed.

SPECT System Description

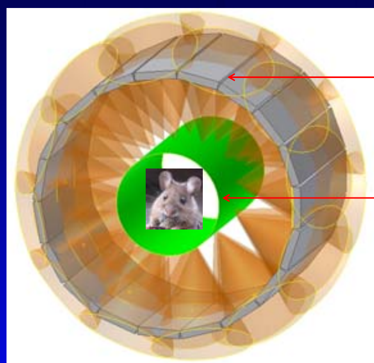

5 rings of 19 CZT detector modules

Multipinhole collimator

3D drawing of the SPECT system

SPECT System Description

Experimental set up with the SPECT system set up with stepper motor and phantom on lab bench

Importance of System Calibration

- Careful system calibration can significantly improve image quality
  - Contrast
  - Resolution
  - Artifact reduction
- Three calibration steps are needed
  - Geometric Calibration
  - Energy Calibration
  - Uniformity Calibration

Geometric Calibration

- Misalignment between detector and multipinhole collimator will cause severe image artifacts
- Co-57 point source scanned at seven positions to measure misalignment
- Measurement included in system matrix used for reconstruction of projection data

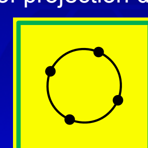

Example four sided detector and 4-pinhole collimator

System Calibration Phantom

- Difficult to study the performance of the ring-type SPECT system with conventional phantoms
- An annular shell phantom with uniform shell thickness was developed for the system calibration
- The phantom was filled with 17µCi of Tc-99m solution in system calibration measurements
- Data acquired in listmode format

(a) Side view, (b) top view of the annular shell phantom and (c) with the phantom inside the SPECT system for system calibration

Energy Calibration

- Energy spectrum variations
  - Found in different detector pixels
  - Also found difference in energy resolution
- Energy calibration method
  - For each detector pixel
    - *Record the energy spectrum separately*
    - *Identify and store energy peak index*
    - *Measure and store FWHM of energy peak*

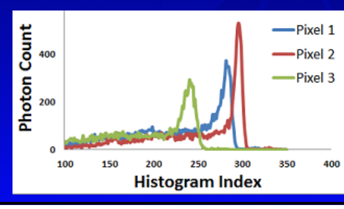

Sample energy spectra from 3 representative pixels

Uniformity Calibration Method

- Obtained flood image of the CZT detector modules using the annular shell phantom
- Positioned the energy window around the energy peak of each detector pixel
- Identified malfunctioning pixels from the processed flood image
  - 0.6% are dead
  - 0.3% are 'hypoactive'
  - 1.1% are 'hyperactive'
- Replaced values of malfunctioned pixels with zeros and stored locations of pixels
- Generated uniformity correction map with flood image

System Calibration Procedure

- The experimentally acquired projection data were processed with the following procedure
  - Counts extracted from listmode data using stored energy windows to generate initial image
  - Uniformity map applied to initial image
  - Values of stored malfunctioning pixels interpolated from surrounding pixel values

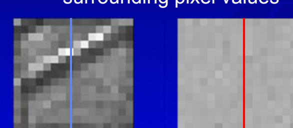

Test flood image (a) before and (b) after uniformity correction from a sample detector module

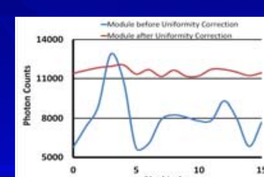

Vertical profile through the sample detector module

Evaluation of System Calibration Method

- Acquired projection data from a uniform cylindrical and a hot rod phantom using a 36-pinhole collimator at two collimator positions
- Images reconstructed using a 3D ML-EM image reconstruction method with modeled collimator detector response
- Assessed quality of the MPH SPECT images

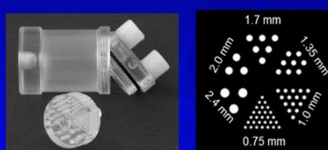

(a) (b)

(a) Photo and (b) schematic diagram of the cross-section of a Data Spectrum Hot Rod phantom

Effect of Geometric Calibration

- SPECT images with and without geometric misalignment measurement included in system matrix
- Artifacts dominate image if misalignment measurement not included

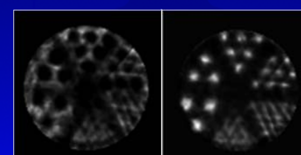

Reconstructed rod phantom image without (left) and with (right) geometric misalignment correction

Effect of Energy Calibration

- SPECT images of the hot rod phantom with and without energy calibration
- Results show ~40% improvement in image contrast

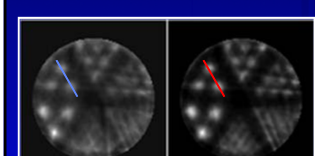

(a) (b)

SPECT images from hot rod phantom(a) without and (b) with energy calibration. Projection data acquired using a 36-pinhole collimator

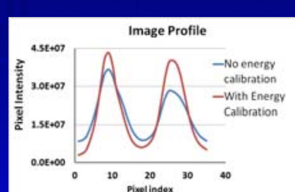

Sample profiles through the SPECT SPECT images

Effect of Uniformity Calibration

Uniform Phantom Without Uniformity Calibration

Initial 36-pinhole projection image of uniform cylinder

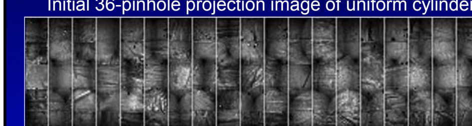

Reconstructed image

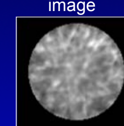

- Raw 36-pinhole projection image from the uniform cylinder shows many nonuniformities
- Reconstructed image shows many artifacts
- Integral uniformity in reconstructed image: 37.5%

Effect of Uniformity Calibration

After application of uniformity correction map

Uniformity corrected 36-pinhole projection image

Reconstructed image

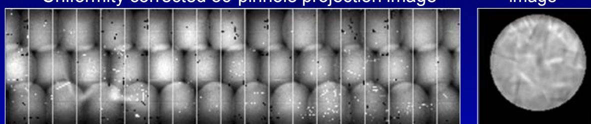

- Hot and cold pixels remain in projection image
- Reconstructed image is improved, but still has several artifacts
- Integral uniformity in reconstructed image: 28.3%

Effect of Uniformity Calibration

After application of uniformity correction map and malfunctioning pixel correction

Final corrected 36-pinhole projection image

Reconstructed image

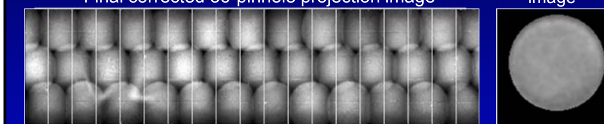

- Projection image has very few (if any) nonuniformities
- Reconstructed image is artifact free
- Integral uniformity in reconstructed image: 5.9%

Effect of Uniformity Calibration

Rod Phantom Without Uniformity Calibration

Initial 36-pinhole projection image of uniform cylinder

Reconstructed image

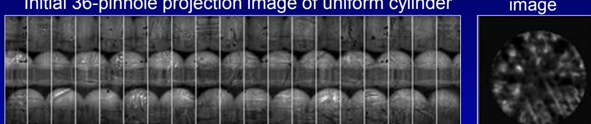

- Initial projection image of rod phantom has many nonuniformities
- Reconstructed image has streaking artifacts and rods have nonuniform pixel values
- Only 2.4mm, 2mm, and 1.7mm rods can be resolved

Effect of Uniformity Calibration

After application of uniformity correction map

Uniformity corrected 36-pinhole projection image

Reconstructed image

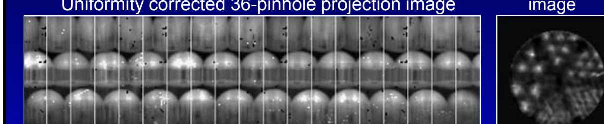

- Projection image still has hot and cold pixels
- Reconstructed image has less streaking, still has nonuniformities in rods
- 2.4mm, 2mm, and 1.7mm resolved, 1.35mm rods mostly resolved

Effect of Uniformity Calibration

After application of uniformity correction map and malfunctioning pixel correction

Final corrected 36-pinhole projection image

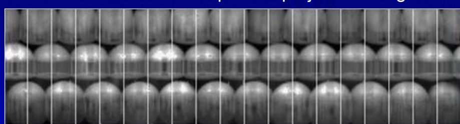

Reconstructed image

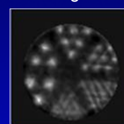

- Projection image has few (if any) nonuniformities
- Reconstructed image is artifact free
- 2.4mm, 2mm, 1.7mm, and 1.35 rods resolved, 1mm rods partially resolved

Conclusions

- We have developed and tested a simple and repeatable system calibration method that allows our CZT detector based SPECT system produce artifact free 3D multipinhole images with high image quality
- The system calibration method allows much improved MPH SPECT image quality in terms of
  - Contrast
  - Resolution
  - Reduction in image artifacts

Acknowledgments

- This research was supported by the NIH research grant R01 EB 008730

Thank you!